Biochemical and Biophysical Research Communications 453 (2014) 686–691

Contents lists available at ScienceDirect

Biochemical and Biophysical Research Communications

journal homepage: www.elsevier.com/locate/ybbrc

A model for the coordinated stepping of cytoplasmic dynein

X.Y. Zhao [a,b], W. Sun [a,c], J.P. Zhang [a], Tala [a], W.S. Guo [a,*]

[a] School of Physical Science and Technology, Inner Mongolia University, 235 West Street, 010021 Hohhot, Inner Mongolia, China
[b] Inner Mongolia Vocational College of Chemical Engineering, Higher Vocational Technology Park, 010070 Hohhot, Inner Mongolia, China
[c] Department of Information and Automation, Ordos Vocational College, Yikezhao Street, Kangbashi New District, 017000 Ordos, Inner Mongolia, China

ARTICLE INFO

Article history:
Received 5 September 2014
Available online 6 October 2014

Keywords:
Cytoplasmic dynein complex
Mechanochemical cycle
Elastic linkage
Step size distribution
Striding rate

ABSTRACT

Cytoplasmic dynein play an important role in transporting various intracellular cargos by coupling their ATP hydrolysis cycle with their conformational changes. Recent experimental results showed that the cytoplasmic dynein had a highly variable stepping pattern including "hand-over-hand", "inchworm" and "nonalternating-inchworm". Here, we developed a model to describe the coordinated stepping patterns of cytoplasmic dynein, based on its working cycle, construction and the interaction between its leading head and tailing head. The kinetic model showed how change in the distance between the two heads influences the rate of cytoplasmic dynein under different stepping patterns. Numerical simulations of the distribution of step size and striding rate are in good quantitative agreement with experimental observations. Hence, our coordinated stepping model for cytoplasmic dynein successfully explained its diverse stepping patterns as a molecular motor. The cooperative mechanism carried out by the two heads of cytoplasmic dynein shed light on the strategies adopted by the cytoplasmic dynein in executing various functions.

1. Introduction

Cytoplasmic dynein is a complex and microtubule-based molecular motor [1]. It can use the free energy of ATP hydrolysis to produce mechanical work and drive a variety of fundamental cellular processes, including cellular organelle transport, mitotic spindle positioning, and nuclear segregation [2–5]. In the past fifty years, the molecular structure, physiological functions and regulation mechanism of cytoplasmic dynein have been well documented [6]. Currently, cytoplasmic dynein is at the frontier of cell motility research at the molecular level, as its mechanism of movement is poorly understood [6].

The cytoplasmic dynein complex is composed of two identical heavy chains and several smaller associated polypeptides [7–9]. The molecular mass of each heavy chain is typically 500–540 kDa, with approximately 4500 amino acid residues. The heavy chain consists of three major parts: the AAA ring head, the stalk, and the tail. The head serving as the catalytic engine of the motor, contains six AAA modules (AAA1–AAA6) tandemly arranged in a ring, and it is structurally related to hexameric ATPases in the AAA + superfamily [2,10–12]. The first four AAA modules (AAA1–4) contain nucleotide-binding and hydrolysis Walker A motifs. Among them, AAA1 is the primary site for ATP hydrolysis and dynein motility [13] although the other three sites (AAA2–4) also bind nucleotides and may contribute important regulatory functions [14–16]. AAA5 and AAA6 have lost their conserved nucleotide binding sites and are thought to serve structural roles [17]. Linker, which has been proposed to serve as a mechanical element, is a structure connecting AAA1 and the main part of the tail [17–21]. The tails of the two heads acts as a scaffold for assembly of different intermediate chains and light intermediate chains to form the dynein complex [22]. The stalk emerging from between AAA4 and AAA5 is a ~15 nm anti-paralleled coiled-coil [18,19]. A globular microtubule-binding domain is located at its tip [23].

A number of significant conclusions about cytoplasmic dynein's kinetic characteristic and mechanism have been obtained. By using optical-trap measurement, Mallik et al. [24] found that under no load the step size of dynein was predominantly 24–32 nm and the force produced was about 0.28 pN. With the increase of load applied to dynein, the step size decreased gradually to 8 nm and the force produced was up to 1.1 pN. Based on the observation that the correlation between force production and step size is consistent with a molecular gear mechanism, they proposed a dynein's gear model. According to this model, increasing load induces the binding of ATP at secondary sites in the dynein head, which makes

* Corresponding author at: School of Physical Science and Technology, Inner Mongolia University, 235 West Street, 010021 Hohhot City, Inner Mongolia, China. Fax: +86 471 4992922.
E-mail address: pygws@imu.edu.cn (W.S. Guo).

http://dx.doi.org/10.1016/j.bbrc.2014.09.138
0006-291X/

dynein take smaller but more powerful stroke at a high load condition. Shima et al. [25] found that the coordination of its two heads is necessary for a processive motion of cytoplasmic dynein. They also noticed that the two head of a cytoplasmic dynein complex communicated with each other to move processively, and both motor domains could not dissociate from the microtubule simultaneously. Reck-Peterson et al. [26] found that cytoplasmic dynein complex moved forward prominently with 8 nm step although longer steps as well as side and backward movement were observed. They thought that dynein's variable step sizes and directions were a considerable diffusional component to its step. Walter et al. [27] reported that dynein complex itself was capable of moving in either direction of the microtubule i.e., towards the plus or towards the minus end, but macroscopically towards the minus end. Distinct from kinesin and myosin, both of which use "hand-over-hand" mechanism, Qiu et al. [28] reported that the cytoplasmic dynein complex had a variable stepping pattern by mixing of "hand-over-hand", "inchworm" and "unalternating-inchworm". Basically, the "hand-over-hand" means that two heads alternate their steps passing the other head in space in every step. "Inchworm" means that two heads alternate their steps and don't step passing the other head in space in every step. "Unalternating-inchworm" means that one head could take multiple consecutive steps before the other head moved [20].

Although variable stepping patterns of cytoplasmic dynein had been observed experimentally, at present no mathematical model capable of explaining the coordinated stepping patterns of cytoplasmic dynein has been reported yet. Based on the mechanochemical cycle model of dynein, the structure of cytoplasmic dynein complex and the interaction of its two heads, we developed a mathematical theory for cytoplasmic dynein's coordinated stepping. We analyzed cytoplasmic dynein's moving patterns including "hand-over-hand", "inchworm" and "unalternating-inchworm" and their key features including the distribution of stepping size and striding rate. Our results provide insight into the mechanism of cytoplasmic dynein movement and may help to explain various functions that cytoplasmic dynein executes.

2. Methods

2.1. Model for coordinated stepping of cytoplasmic dynein

Based on the results of the experiments for dynein monomers binding to microtubule, Imamula et al. proposed a mechanochemical ATPase cycle for single dynein head [8,29]. The model consists of the following steps. (1) The empty (nucleotide-free) head strongly interacts with the microtubule. (2) ATP binding to an empty head causes the head dissociation from the microtubule (or weak association) and generates conformational change. The dynein adopts a prepower-stroke configuration (recovery). (3) After ATP hydroxylation the inorganic phosphate is released and the free head binds strongly to the microtubule again. The head undergoes a conformational change (power stroke) to the postpower-stroke state. (4) Finally, ADP is released representing the completion of the cycle [8,29].

The model was simplified as follows:

$$\text{Dynein}\cdot\text{M}+\text{ATP}\xrightarrow{k_d}\text{Dynein}\cdot\text{ATP}+\text{M}$$

$$\text{Dynein}\cdot\text{ATP}+\text{M}\xrightarrow{k_a}\text{Dynein}\cdot\text{M}+\text{ADP}+\text{Pi}$$

M: microtubule, Dynein·M: dynein binding to microtubule, Dynein·ATP: ATP binding to dynein. Let k_d denote the dissociation rate of the head from the microtubule and k_a for the association rate of the head to the microtubule.

We make two assumptions: (1) both heads of dynein could not dissociate from microtubule spontaneously; (2) the linkage between the two heads of the cytoplasmic dynein is elastic. A model for coordinated stepping of cytoplasmic dynein is suggested as Fig. 1.

There are two possible ways for cytoplasmic dynein complex to complete mechanochemical ATPase cycle. Fig. 1A shows the cycle of the leading head. After dissociation from microtubule, the leading head can bind to any binding site with different probability. If the leading head binds to site 3, 4, 5, 6..., the dynein complex moves towards the minus end of microtubule. This form of motion is represented by A1. If it binds to site 2, 1, −1, −2, −3..., the dynein complex moves towards the plus end. This form of motion is presented by A2, in which binding to site −1, −2, −3... indicates that the leading head passes the trailing head in space.

Fig. 1B shows the cycle of the trailing head. After dissociation from microtubule, the trailing head can bind to any of the binding site with different probability. If the trailing head binds to site 1, 2, 4, 5, 6..., the dynein complex moves towards the minus end of the microtubule. This form of motion is represented by B1. Among them, binding to site 4, 5, 6... indicates that the trailing head passes the leading head in space. On the other hand, binding to site 2, 1, −1, −2, −3... means that the dynein complex moves towards the plus end of microtubule. This form of motion is represented as B2. Let k_{df}' denote the dissociation rate from the microtubule of the leading head, k_{db}' for the dissociation rate of the trailing head, k_{af}' for the association rate binding for the front site compared to the site before dissociation, and k_{ab}' for the association rate for the back site.

2.2. Analysis of the step-size distribution and the striding rate

To obtain the step-size distribution and the striding rate, the dissociation and association rates k_{df}', k_{db}', k_{af}', k_{ab}' were calculated from the model in Fig. 1.

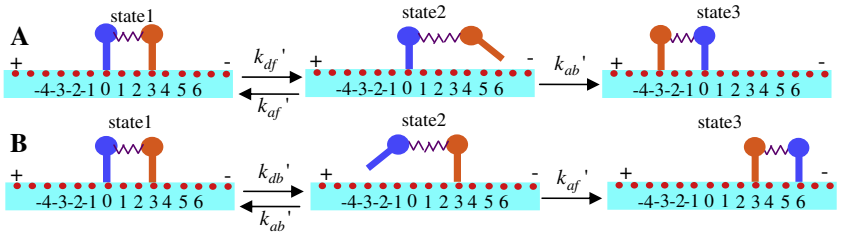

Fig. 1. Stepping patterns for cytoplasmic dynein complex. (A) The schematic representation of the leading head stepping. (B) The schematic representation of the trailing head stepping. In state 1, two heads bind to microtubule spontaneously. The numbered red dots represent dynein binding sites, red head represents leading head and blue head denotes trailing head. The linkage is represented with elastic element. Assume the linkage is at relaxation (non-force-generating) state when the two heads are three sites apart. + and − represent the plus and minus end of the microtubule, respectively. (For interpretation of the references to color in this figure legend, the reader is referred to the web version of this article.)

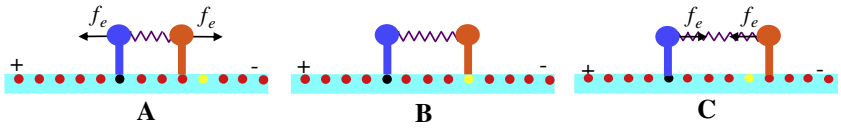

Fig. 2. The schematic representation of the relative position of the two heads. The blue head is the trailing head; the red head is the leading head. The black and yellow sites represent the relative equilibrium sites of the two heads. The elastic element length between the two head is l and balanced length is b. (A) $l < b$, elastic force applied on the leading head is in the direction of the minus end of the microtubule, while applied on the trailing head is in the direction of the plus end of microtubule. (B) $l = b$, there is no elastic force applied on either leading head or trailing head. (C) $l > b$, elastic force applied on the leading head is in the direction of the plus end of the microtubule, while applied on the trailing head is in the direction of the minus end of the microtubule. (For interpretation of the references to color in this figure legend, the reader is referred to the web version of this article.)

For the three situations shown in Fig. 2, the dissociation rates and association rates of the different motion pattern A1, A2, B1 and B2 can be analyzed using the Bell equation $k = k_0 \exp(\varphi/k_BT)$. Where k_0 denotes rate constant in equilibrium state, φ is energy including the chemical energy from ATP hydrolyzation and elastic potential energy of the linkage between the two heads.

The dynein heads always walk along different protofilaments [22], the on-axis (parallel to the microtubule along axis) step size could not be the integral multiple of 8 nm. To simplify the model, in the following the step size was chosen as integral multiple of 4 nm.

2.2.1. In the state 2A ($l < b$)

When dynein hydrolyzes ATP and adopts pattern A, according to Bell equation, k_{df}', k_{af}' and k_{ab}' should be

$$k'_{df} = k_{df} \exp\left(\frac{G_1 + \frac{1}{2}\lambda(l-b)^2}{k_BT}\right) \tag{1}$$

$$k'_{af} = k_{af} \exp\left(\frac{-\frac{1}{2}\lambda\Delta x'^2}{k_BT}\right) = k_{af} \exp\left(\frac{-\frac{1}{2}\lambda(d+l-b)^2}{k_BT}\right),$$
$$d = 4,\ 8,\ 12,\ 16,\ldots \tag{2}$$

$$k'_{ab} = k_{ab} \exp\left(\frac{-\frac{1}{2}\lambda\Delta x'^2}{k_BT}\right) = k_{ab} \exp\left(\frac{-\frac{1}{2}\lambda(d+l-b)^2}{k_BT}\right),$$
$$d = -4,\ -8,\ -12,\ldots \tag{3}$$

The chemical energy from ATP hydrolyzation ΔG_0(= 49.83 pN nm) can be divided into two parts: G_1 is used to dissociate the head from microtubule; G_2 is the conformational energy stored in dynein. When the trailing head dissociates from the microtubule, the conformational energy stored in the leading head facilitates the trailing head to move towards the minus end of the microtubule [30]. In the situation of Fig. 2A, the elastic element is compressed, the elongation is $\Delta x = l - b$, the elastic coefficient of the elastic element is λ, and elastic potential energy in the elastic element is $\frac{1}{2}\lambda(l-b)^2$. In the cycle of pattern A1, let the step size of leading head be d, $d = \ldots -16$ nm, -12 nm, -8 nm, -4 nm or $d = 0$ nm, 4 nm, 8 nm, 12 nm, 16 nm…. The elastic element is compressed or stretched and the elongation is $\Delta x' = d + \Delta x$, elastic potential energy is $\frac{1}{2}\lambda(d+l-b)^2$. The rate that dynein finishes cycle of pattern A1 is:

$$k_{f(+d)} = k'_{df}k'_{af} = k_{df}k_{af} \exp\left(\frac{G_1 + \frac{1}{2}\lambda(l-b)^2 - \frac{1}{2}\lambda(d+l-b)^2}{k_BT}\right),$$
$$d = 4,\ 8,\ 12,\ 16,\ldots \tag{4}$$

The subscript f of $k_{f(+d)}$ denotes the move of leading head and $+d$ denotes that the direction of the motion is towards the minus end of the microtubule.

The rate that dynein finishes cycle of pattern A2 is:

$$k_{f(-d)} = k'_{df}k'_{ab} = k_{df}k_{ab} \exp\left(\frac{G_1 + \frac{1}{2}\lambda(l-b)^2 - \frac{1}{2}\lambda(d+l-b)^2}{k_BT}\right),$$
$$d = -4,\ -8,\ -12,\ -16,\ldots \tag{5}$$

The subscript f of $k_{f(-d)}$ denotes the move of leading head, $-d$ denotes that the direction of the motion is towards the plus end of the microtubule.

When dynein hydrolyzes ATP and adopts pattern B, according to Bell equation, k_{db}', k_{af}' and k_{ab}' should be

$$k'_{db} = k_{db} \exp\left(\frac{G_1 - \frac{1}{2}k(l-b)^2}{k_BT}\right) \tag{6}$$

$$k'_{af} = k_{af} \exp\left(\frac{G_2 - \frac{1}{2}k\Delta x'^2}{k_BT}\right) = k_{af} \exp\left(\frac{G_2 - \frac{1}{2}k(d+l-b)^2}{k_BT}\right),$$
$$d = 4,\ 8,\ 12,\ 16,\ldots \tag{7}$$

$$k'_{ab} = k_{ab} \exp\left(\frac{-G_2 - \frac{1}{2}k\Delta x'^2}{k_BT}\right) = k_{ab} \exp\left(\frac{-G_2 - \frac{1}{2}k(d+l-b)^2}{k_BT}\right),$$
$$d = -4,\ -8,\ -12,\ -16,\ldots \tag{8}$$

The rate that dynein finishes cycle of pattern B1 is:

$$k_{b(+d)} = k'_{db}k'_{af} = k_{db}k_{af} \exp\left(\frac{G_1 + G_2 - \frac{1}{2}\lambda(l-b)^2 - \frac{1}{2}\lambda(d+l-b)^2}{k_BT}\right),$$
$$d = 4,\ 8,\ 12,\ 16,\ldots \tag{9}$$

The subscript b of $k_{b(+d)}$ denotes the move of trailing head, $+d$ denotes that the direction of the motion is towards the minus end of the microtubule.

The rate that dynein finish cycle of pattern B2 is:

$$k_{b(-d)} = k'_{db}k'_{ab} = k_{db}k_{ab} \exp\left(\frac{G_1 - G_2 - \frac{1}{2}\lambda(l-b)^2 - \frac{1}{2}\lambda(d+l-b)^2}{k_BT}\right),$$
$$d = -4,\ -8,\ -12,\ -16,\ldots \tag{10}$$

The subscript b of $k_{b(-d)}$ denotes that the trailing head moves, $-d$ denotes that the direction of the motion is towards the plus end of the microtubule.

2.2.2. In the state 2B ($l = b$)

(1) When dynein hydrolyzes ATP and adopts pattern A, according to Bell equation, k_{df}', k_{af}' and k_{ab}' should be

$$k'_{df} = k_{df} \exp\left(\frac{G_1}{k_BT}\right) \tag{11}$$

$$k'_{af} = k_{af} \exp\left(\frac{-\frac{1}{2}\lambda\Delta x'^2}{k_BT}\right) = k_{af} \exp\left(\frac{-\frac{1}{2}\lambda d^2}{k_BT}\right),$$
$$d = 4,\ 8,\ 12,\ 16,\ldots \tag{12}$$

$$k'_{ab} = k_{ab}\exp\left(\frac{-\frac{1}{2}\lambda\Delta x'^2}{k_BT}\right) = k_{ab}\exp\left(\frac{-\frac{1}{2}\lambda d^2}{k_BT}\right),$$
$$d = -4,\ -8,\ -12,\ldots \tag{13}$$

The rate that dynein finishes cycle of pattern A1 is:

$$k_{f(+d)} = k'_{df}k'_{af} = k_{df}k_{af}\exp\left(\frac{G_1 - \frac{1}{2}\lambda d^2}{k_BT}\right),$$
$$d = 4,\ 8,\ 12,\ 16,\ldots \tag{14}$$

The rate that dynein finishes cycle of pattern A2 is:

$$k_{f(-d)} = k'_{df}k'_{ab} = k_{df}k_{ab}\exp\left(\frac{G_1 - \frac{1}{2}\lambda d^2}{k_BT}\right),$$
$$d = -4, -8, -12, -16\ldots \tag{15}$$

(2) When dynein hydrolyzes ATP and adopts pattern B, according to Bell equation, k_{df}', k_{af}' and k_{ab}' should be

$$k'_{db} = k_{db}\exp\left(\frac{G_1}{k_BT}\right) \tag{16}$$

$$k'_{af} = k_{af}\exp\left(\frac{G_2 - \frac{1}{2}\lambda\Delta x'^2}{k_BT}\right) = k_{af}\exp\left(\frac{G_2 - \frac{1}{2}\lambda d^2}{k_BT}\right),$$
$$d = 4,\ 8,\ 12,\ 16,\ldots \tag{17}$$

$$k'_{ab} = k_{ab}\exp\left(\frac{-G_2 - \frac{1}{2}\lambda\Delta x'^2}{k_BT}\right) = k_{ab}\exp\left(\frac{-G_2 - \frac{1}{2}\lambda d^2}{k_BT}\right),$$
$$d = -4,\ -8,\ -12,\ldots \tag{18}$$

The rate that dynein finishes cycle of pattern B1 is:

$$k_{b(+d)} = k'_{db}k'_{af} = k_{db}k_{af}\exp\left(\frac{G_1 + G_2 - \frac{1}{2}\lambda d^2}{k_BT}\right),$$
$$d = 4,\ 8,\ 12,\ 16,\ldots \tag{19}$$

The rate that dynein finishes cycle of pattern B2 is:

$$k_{b(-d)} = k'_{db}k'_{ab} = k_{db}k_{ab}\exp\left(\frac{G_1 - G_2 - \frac{1}{2}\lambda d^2}{k_BT}\right),$$
$$d = -4,\ -8,\ -12,\ -16,\ldots \tag{20}$$

2.2.3. In the state 2C (l > b)

(1) When dynein hydrolyzes ATP and adopts pattern A, according to Bell equation, k_{df}', k_{af}' and k_{ab}' should be

$$k'_{df} = k_{df}\exp\left(\frac{G_1 - \frac{1}{2}\lambda(l-b)^2}{k_BT}\right) \tag{21}$$

$$k'_{af} = k_{af}\exp\left(\frac{-\frac{1}{2}\lambda\Delta x'^2}{k_BT}\right) = k_{af}\exp\left(\frac{-\frac{1}{2}\lambda(d+l-b)^2}{k_BT}\right),$$
$$d = 4,\ 8,\ 12,\ 16,\ldots \tag{22}$$

$$k'_{ab} = k_{ab}\exp\left(\frac{\frac{1}{2}\lambda\Delta x'^2}{k_BT}\right) = k_{ab}\exp\left(\frac{\frac{1}{2}\lambda(d+l-b)^2}{k_BT}\right),$$
$$d = -4,\ -8,\ -12,\ldots \tag{23}$$

The rate that dynein finishes cycle of pattern A1 is:

$$k_{f(+d)} = k'_{df}k'_{af} = k_{df}k_{af}\exp\left(\frac{G_1 - \frac{1}{2}\lambda(l-b)^2 - \frac{1}{2}\lambda(d+l-b)^2}{k_BT}\right),$$
$$d = 4,\ 8,\ 12,\ 16,\ldots \tag{24}$$

The rate that dynein finishes cycle of pattern A2 is:

$$k_{f(-d)} = k'_{df}k'_{ab} = k_{df}k_{ab}\exp\left(\frac{G_1 - \frac{1}{2}\lambda(l-b)^2 - \frac{1}{2}\lambda(d+l-b)^2}{k_BT}\right),$$
$$d = -4,\ -8,\ -12,\ -16,\ldots \tag{25}$$

(2) When dynein hydrolyzes ATP and adopts pattern B, according to Bell equation, k_{db}', k_{af}' and k_{ab}' should be

$$k'_{db} = k_{db}\exp\left(\frac{G_1 + \frac{1}{2}\lambda(l-b)^2}{k_BT}\right) \tag{26}$$

$$k'_{af} = k_{af}\exp\left(\frac{G_2 - \frac{1}{2}\lambda\Delta x'^2}{k_BT}\right) = k_{af}\exp\left(\frac{G_2 - \frac{1}{2}\lambda(d+l-b)^2}{k_BT}\right),\quad d = 4,\ 8,\ 12,\ 16,\ldots \tag{27}$$

$$k'_{ab} = k_{ab}\exp\left(\frac{-G_2 - \frac{1}{2}\lambda\Delta x'^2}{k_BT}\right) = k_{ab}\exp\left(\frac{-G_2 - \frac{1}{2}\lambda(d+l-b)^2}{k_BT}\right),$$
$$d = -4,\ -8,\ -12,\ -16,\ldots \tag{28}$$

The rate that dynein finishes cycle of pattern B1 is:

$$k_{b(+d)} = k'_{db}k'_{af} = k_{db}k_{af}\exp\left(\frac{G_1 + G_2 + \frac{1}{2}\lambda(l-b)^2 - \frac{1}{2}\lambda(d+l-b)^2}{k_BT}\right),$$
$$d = 4,\ 8,\ 12,\ 16,\ldots \tag{29}$$

The rate that dynein finishes cycle of pattern B2 is:

$$k_{b(-d)} = k'_{db}k'_{ab} = k_{db}k_{ab}\exp\left(\frac{G_1 - G_2 + \frac{1}{2}\lambda(l-b)^2 - \frac{1}{2}\lambda(d+l-b)^2}{k_BT}\right),$$
$$d = -4,\ -8,\ -12,\ -16,\ldots \tag{30}$$

3. Results and discussion

The elastic element length between the two heads of cytoplasmic dynein is l and balanced length is b. According to Eqs. (4), (5), (9), (10), (14), (15), (19), (20), (24), (25), (29), (30) we calculated the rate $k_{f(+d)}$, $k_{f(-d)}$, $k_{b(+d)}$ and $k_{b(+d)}$ for a given l. The rate $k_{f(+d)}$, $k_{f(-d)}$, $k_{b(+d)}$ and $k_{b(+d)}$ was converted into the probabilities. For a given l, the probabilities of step size $+d$ or $-d$, q_{+d} and q_{-d}, were calculated by

$$q_{+d} = \frac{1}{2}\left(\frac{k_{f(+d)}}{\sum^{l}_{d=\ldots,-12,\ -8,\ -4,\ 0,\ 4,\ 8,\ 12,\ldots}\left(k_{f(+d)} + k_{f(-d)}\right)} + \frac{k_{b(+d)}}{\sum^{l}_{d=\ldots,-12,\ -8,\ -4,\ 0,\ 4,\ 8,\ 12,\ldots}\left(k_{b(+d)} + k_{b(-d)}\right)}\right) \tag{31}$$

$$q_{-d} = \frac{1}{2}\left(\frac{k_{f(-d)}}{\sum^{l}_{d=\ldots,-12,\ -8,\ -4,\ 0,\ 4,\ 8,\ 12,\ldots}\left(k_{f(+d)} + k_{f(-d)}\right)} + \frac{k_{b(-d)}}{\sum^{l}_{d=\ldots,\ -12,\ -8,\ -4,\ 0,\ 4,\ 8,\ 12,\ldots}\left(k_{b(+d)} + k_{b(-d)}\right)}\right) \tag{32}$$

The probabilities of step size $+d$ or $-d$, Q_{+d} and Q_{-d}, were calculated by

$$Q_{+d} = \frac{1}{10}\sum_{l=4,\ 8,\ 12,\ 16,\ 20,\ 24,\ 28,\ 32,\ 36,\ 40}(q_{+d}) \tag{33}$$

$$Q_{-d} = \frac{1}{10}\sum_{l=4,\ 8,\ 12,\ 16,\ 20,\ 24,\ 28,\ 32,\ 36,\ 40}(q_{-d}) \tag{34}$$

Assume that $k_{df} = k_{db}$. Because of the polarity and intrinsic asymmetry of the microtubule, for a certain step size d, k_{af} and k_{ab} are not equal. Based on the experimental result [30], we took $k_{af} \approx 0.86k$, $k_{ab} \approx 0.14k$ (k is a constant). ΔG_0 is the free energy of ATP hydrolyzing. $k_BT = 4.1$ pN nm. k_B is the Boltzmann constant and T is absolute temperature. λ is the elastic coefficient of the elastic element, valued 0.14 pN/nm. The length change of the elastic element induced by the conformational change of dynein is 6.28 nm [31], the elastic energy is

$$E = \frac{1}{2}\lambda * 6.28\text{nm}^2 = \frac{1}{2} * 0.14 * 6.28^2 = 2.76\text{pN} \cdot \text{nm} \quad (35)$$

We assume that conformational energy stored in dynein is $G_2 = E$, so

$$G_1 = 49.83 - 2.76 = 47.07\text{pN} \cdot \text{nm} \quad (36)$$

The step-size distribution for the above parameters was shown in Fig. 3.

The numerical calculation showed that, given the elastic coefficient of the linkage λ, the step-size distribution of the cytoplasmic dynein was related to the equilibrium distance b. Because the values of λ and b were not given in the work of Qiu et al. [28], there are some differences between our theoretical results and their experiment data., The distribution of the step size obtained from the model of Fig. 1 is similar to the experimental results. Mallik et al. [24] attributed multiple step-size to the working strategy adopted by the single dynein head and tried to establish a mechanism. The experimental results of Qiu et al. showed that the variable stepping pattern might be the strategy adopted by the cytoplasmic dynein complex in executing various function. The preliminary calculation from this model indicated that the loaded cytoplasmic dynein complex tended to move forwards with the inchworm pattern.

The condition for the leading head passing across the trailing head is that the leading head must move towards the plus end of the microtubule with the step size greater than the distance between the two heads. As shown in Fig. 3, the probability of backward movement is very small, so in the calculation of the striding rate, only the striding rate of the trailing head was considered. The striding rate is a ratio of the probability of the trailing head passing across the leading head to the probability of the trailing head moving. Our calculated striding rate is 16.2% when the equilibrium distance between the two head is $b = 16$ nm (Fig. 4), while the experimental result obtained by Qiu et al. [28] was 17%.

The moving probabilities of the leading head and the trailing head, P_f and P_b, were calculated for different l = 4, 8, 12, 16, 20, 24, 28, 32, 36, 40 nm, as shown in Table 1. The probability of P_f was about half of the value of P_b. In the work of Qiu et al. [28], the ratio of the nonalternating stepping occurred to alternating stepping was 33:67. This suggests the reliability of our model in describing the pattern adopted by cytoplasmic dynein in their processive motion.

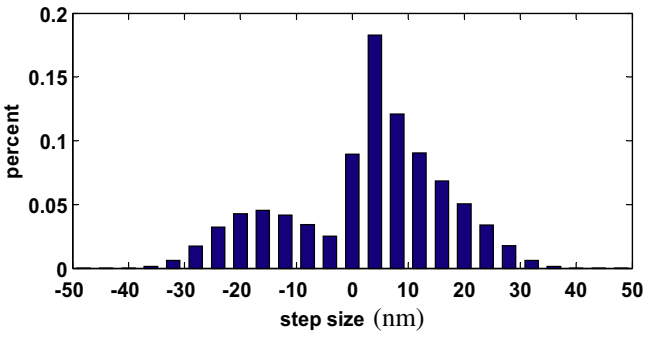

Fig. 3. Histogram of the step size of cytoplasmic dynein complex at $b = 16$ nm.

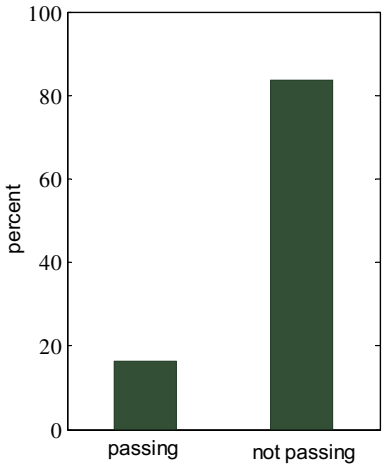

Fig. 4. Spatial analysis of the relative frequency of passing or not passing steps derived from the model.

Table 1
The moving probability of the leading head and the trailing head. ($b = 16$ nm).

l (nm)	4	8	12	16	20	24	28	32	36	40
P_f (%)	99.8	98.4	78.7	60.9	38.9	1.7	0.07	0.001	0	0
P_b (%)	0.2	1.6	21.3	39.1	61.1	98.3	99.93	99.999	100	100

The key of this model is to assume that the linkage between the two heads of the cytoplasmic dynein is elastic. The elastic element makes either of the two heads bind to any site of the microtubule by different probabilities after dissociating from the microtubule. Consequently, cytoplasmic dynein facilitated the "hand-over-hand", "inchworm" and "nonalternating inchworm" stepping patterns.

Two factors were considered in calculation of the step-size distribution and the striding rate. One is that the conformational energy in the leading head is conducive to the forward movement of the trailing head [21,32], which is reflected as G_2 in equation above. The other is that the polarity and the asymmetry of the microtubule help the head moving towards its minus end. However, lacking of definite experimental parameters for these factors makes it difficult to calculate both the step-size distribution and the striding rate.

In summary, we have developed a mathematical model to describe the stepping pattern of cytoplasmic dynein. The model can compellingly explain the moving pattern of "hand-over-hand", "inchworm" and "unalternating-inchworm", and calculated the distribution of the step size and the striding rate that are consistent with the experimental results. In addition, our model is not restricted to describe the known stepping pattern, but also could be applicable to other stepping patterns that would be observed in study.

Acknowledgment

This work was supported by Natural Science Foundation of Inner Mongolia Autonomous Region of China (2011ZD01), National Natural Science Foundation of China (30860075), Natural Science Foundation of Inner Mongolia Autonomous Region of China (2014MS0355) and Research Program of Science and Technology at Universities of Inner Mongolia Autonomous Region (NJZY14012).

References

[1] V.J. Allan, Cytoplasmic dynein, Biochem. Soc. Trans. 39 (2011) 1169–1178.
[2] C. Cho, R.D. Vale, The mechanism of dynein motility: insight from crystal structures of the motor domain, Biochim. Biophys. Acta Mol. Cell Res. 2012 (1823) 182–191.
[3] K.K. Pfister, P.R. Shah, H. Hummerich, A. Russ, J. Cotton, A.A. Annuar, S.M. King, E.M.C. Fisher, Genetic analysis of the cytoplasmic dynein subunit families, PLoS Genet. 2 (2006) 11–26.
[4] K.J. Palmer, H. Hughes, D.J. Stephens, Specificity of cytoplasmic dynein subunits in discrete membrane-trafficking steps, Mol. Biol. Cell 20 (2009) 2885–2899.
[5] B. Wickstead, K. Gull, Dyneins across eukaryotes: a comparative genomic analysis, Traffic 8 (2007) 1708–1721.
[6] A.J. Roberts, T. Kon, P.J. Knight, K. Sutoh, S.A. Burgess, Functions and mechanics of dynein motor proteins, Nat. Rev. Mol. Cell Biol. 14 (2013) 713–726.
[7] S.J. King, M. Bonilla, M.E. Rodgers, T.A. Schroer, Subunit organization in cytoplasmic dynein subcomplexes, Protein Sci. 11 (2002) 1239–1250.
[8] K. Imamula, T. Kon, R. Ohkura, K. Sutoh, The coordination of cyclic microtubule association/dissociation and tail swing of cytoplasmic dynein, Proc. Natl. Acad. Sci. U.S.A. 104 (2007) 16134–16139.
[9] T. Kon, T. Mogami, R. Ohkura, M. Nishiura, K. Sutoh, ATP hydrolysis cycle-dependent tail motions in cytoplasmic dynein, Nat. Struct. Mol. Biol. 12 (2005) 513–519.
[10] A.F. Neuwald, L. Aravi, J.L. Spouge, E.V. Koonin, AAA(+): a class of chaperone-like ATPases associated with the assembly, operation, and disassembly of protein complexes, Genome Res. 9 (1999) 27–43.
[11] R.D. Vale, AAA proteins: Lords of the ring, J. Cell Biol. 150 (2000) F13–F19.
[12] J.P. Erzberger, J.M. Berger, Evolutionary relationships and structural mechanisms of AAA plus proteins, Annu. Rev. Biophys. Biomol. Struct. (2006) 93–114.
[13] B.H. Gibbons, I.R. Gibbons, Vanadate-sensitized cleavage of dynein heavy chains by 365-nm irradiation of demembranated sperm flagella and its effect on the flagellar motility, J. Biol. Chem. 262 (1987) 8354–8359.
[14] T. Kon, M. Nishiura, R. Ohkura, Y.Y. Toyoshima, K. Sutoh, Distinct functions of nucleotide-binding/hydrolysis sites in the four AAA modules of cytoplasmic dynein, Biochemistry 43 (2004) 11266–11274.
[15] C. Cho, S.L. Reck-Peterson, R.D. Vale, Regulatory ATPase sites of cytoplasmic dynein affect processivity and force generation, J. Biol. Chem. 283 (2008) 25839–25845.
[16] A. Silvanovich, M.G. Li, M. Serr, S. Mische, T.S. Hays, The third P-loop domain in cytoplasmic dynein heavy chain is essential for dynein motor function and ATP-sensitive microtubule binding, Mol. Biol. Cell 14 (2003) 1355–1365.
[17] A.P. Carter, C. Cho, L. Jin, R.D. Vale, Crystal structure of the dynein motor domain, Science 331 (2011) 1159–1165.
[18] A.J. Roberts, N. Numata, M.L. Walker, Y.S. Kato, B. Malkova, T. Kon, R. Ohkura, F. Arisaka, P.J. Knight, K. Sutoh, S.A. Burgess, AAA plus ring and linker swing mechanism in the dynein motor, Cell 136 (2009) 485–495.
[19] T. Kon, K. Sutoh, G. Kurisu, X-ray structure of a functional full-length dynein motor domain, Nat. Struct. Mol. Biol. 18 (2011) U626–U638.
[20] A. Houdusse, A.P. Carter, Dynein swings into action, Cell 136 (2009) 395–396.
[21] S.A. Burgess, M.L. Walker, H. Sakakibara, P.J. Knight, K. Oiwa, Dynein structure and power stroke, Nature 421 (2003) 715–718.
[22] H. Sakakibara, K. Oiwa, Molecular organization and force-generating mechanism of dynein, FEBS J. 278 (2011) 2964–2979.
[23] M.P. Koonce, Identification of a microtubule-binding domain in a cytoplasmic dynein heavy chain, J. Biol. Chem. 272 (1997) 19714–19718.
[24] R. Mallik, B.C. Carter, S.A. Lex, S.J. King, S.P. Gross, Cytoplasmic dynein functions as a gear in response to load, Nature 427 (2004) 649–652.
[25] T. Shima, K. Imamula, T. Kon, R. Ohkura, K. Sutoh, Head-head coordination is required for the processive motion of cytoplasmic dynein, an AAA(+) molecular motor, J. Struct. Biol. 156 (2006) 182–189.
[26] S.L. Reck-Peterson, A. Yildiz, A.P. Carter, A. Gennerich, N. Zhang, R.D. Vale, Single-molecule analysis of dynein processivity and stepping behavior, Cell 126 (2006) 335–348.
[27] W.J. Walter, M.P. Koonce, B. Brenner, W. Steffen, Two independent switches regulate cytoplasmic dynein's processivity and directionality, Proc. Natl. Acad. Sci. U.S.A. 109 (2012) 5289–5293.
[28] W. Qiu, N.D. Derr, B.S. Goodman, E. Villa, D. Wu, W. Shih, S.L. Reck-Peterson, Dynein achieves processive motion using both stochastic and coordinated stepping, Nat. Struct. Mol. Biol. 19 (2012) 193–200.
[29] D. Tsygankov, A.W.R. Serohijos, N.V. Dokholyan, T.C. Elston, Kinetic models for the coordinated stepping of cytoplasmic dynein, J. Chem. Phys. 130 (2009).
[30] M.A. DeWitt, A.Y. Chang, P.A. Combs, A. Yildiz, Cytoplasmic Dynein Moves Through Uncoordinated Stepping of the AAA plus Ring Domains, Science 335 (2012) 221–225.
[31] C.B. Lindemann, A.J. Hunt, Does axonemal dynein push, pull, or oscillate?, Cell Motil Cytoskelet. 56 (2003) 237–244.
[32] S.A. Burgess, M.L. Walker, H. Sakakibara, K. Oiwa, P.J. Knight, The structure of dynein-c by negative stain electron microscopy, J. Struct. Biol. 146 (2004) 205–216.